OXYGEN IONIC AND ELECTRONIC TRANSPORT IN APATITE CERAMICS

A.L. Shaula[a], V.V. Kharton[a], J.C. Waerenborgh[b], D.P. Rojas[b], F.M.B. Marques[a]

[a] Department of Ceramics and Glass Engineering, CICECO, University of Aveiro, 3810-193 Aveiro, Portugal

[b] Chemistry Department, Instituto Tecnológico e Nuclear, Estrada Nacional 10, P-2686-953 Sacavém, Portugal

Abstract

The development of novel oxygen-ion conducting solid electrolytes is of great interest for high-temperature electrochemical applications such as solid oxide fuel cells (SOFCs). This work was focused on the study of transport properties of apatite-type $La_{10}Si_{6-x}Fe_xO_{27-x/2}$ (x = 1–2). Single-phase apatite ceramics with density higher than 98% were prepared by the standard solid-state synthesis route and characterized by X-ray diffraction, dilatometry, impedance spectroscopy, faradaic efficiency (to determine ion transference numbers), and measurements of total conductivity and Seebeck coefficient as function of the oxygen partial pressure varying in the range 10^{-16} Pa to 50 kPa. The ionic conductivity of apatite phases was found to increase with oxygen content. In air, the ion transference numbers of $La_{10}Si_{6-x}Fe_xO_{27-x/2}$ (x= 1.0–1.5) at 700-950°C are higher than 0.99, whilst the p-type electronic contribution to the total conductivity of $La_{10}Si_4Fe_2O_{26}$ is about 3%. Mössbauer spectroscopy showed that the coordination of iron cations, which are all trivalent within the detection limits, increases with oxygen intercalation in the lattice. Reducing $p(O_2)$ below 10^{-8} Pa leads to a decrease in the ionic transport and growing n-type electronic contribution, the role of which increases with iron additions. The average thermal expansion coefficients in air are $(8.2\text{-}9.9)\times10^{-6}$ K^{-1} at 100-1000°C.

Keywords: C. Electrical conductivity; C. Ionic conductivity; C. Thermal expansion; D. Apatite; E. Fuel cells

1. Introduction

Oxide materials with predominant oxygen ionic conductivity attract great attention for high-temperature electrochemical applications, such as solid oxide fuel cells (SOFCs), oxygen sensors and pumps.[1] Solid oxide electrolytes should meet numerous requirements, in particular should exhibit a high ionic conductivity, minimum electronic transport, moderate thermal expansion and thermodynamic stability in wide ranges of oxygen partial pressure and temperature. Moreover, the costs associated with raw materials and processing technologies should be as low as possible. Recently, a substantial level of oxygen ionic transport was reported for lanthanum silicate-based apatite type phases $La_{10-y}Si_6O_{26\pm\delta}$, and their rare earth- and alkaline earth-containing analogues.[2-7] The apatite structure may be described as a framework of isolated SiO_4 tetrahedra, with cavities occupied by La^{3+} or other A-site cations. The maximum ionic conductivity, significantly due to oxygen migration through channels in the lattice, is observed for oxygen-excess compositions. As an example, the ionic transport in $La_{10-y}Si_6O_{26\pm\delta}$ (y= 0.67-2.0) is considerably lower than that in $La_{10}Si_6O_{27}$.[3,4] This phenomenon suggests that the transport of oxygen interstitials is faster than vacancy migration. A significant disorder in the oxygen channels was revealed in oxygen-stoichiometric materials such as $La_{9.33}Si_6O_{26}$, leading to the formation of Frenkel-type defects and a higher ionic conduction with respect to the phases where these channels are ordered.[5] Doping with transition metals such as Fe makes it possible to improve the sinterability of apatite ceramics, whilst the conductivity remains predominantly ionic at oxygen partial pressures from 10^{-2} Pa to 100 kPa, at least for one iron cation per unit formula.[6,7] Continuing our research on apatite-type solid electrolytes[7], the present work was focused on the study of iron-substituted $La_{10}Si_{6-x}Fe_xO_{27-x/2}$ (x = 1-2).

2. Experimental

Dense single-phase $La_{10}Si_{6-x}Fe_xO_{27-x/2}$ ceramics were prepared by a standard solid-state synthesis route from stoichiometric amounts of high-purity La_2O_3, SiO_2 and $Fe(NO_3)_3 \bullet 9H_2O$. Following pre-reaction at 1000-1200^{o}C and ball-milling, ceramic samples were sintered at 1500-1600^{o}C during 10 hours in air. The sintering temperatures are listed in Table 1. Before characterization, all materials were annealed in air at 1000^{o}C for 2-3 hours and then slowly cooled in order to obtain equilibrium oxygen nonstoichiometry. The density of gas-tight samples was higher than 98% of their theoretical density (Table 1).

The X-ray diffraction (XRD) patterns were collected at room temperature using a Rigaku D/MAX-B diffractometer (CuK_α, 2Θ = 10-100˚, step 0.02˚, 1 s/step). Thermal expansion in air was measured by a Linseis L70 dilatometer (heating of 5 K/min). The total conductivity (σ) at 300-1100^{0}C in air was determined by impedance spectroscopy using a HP4284A precision LCR meter (20 Hz - 1 MHz). Also, isothermal measurements of total conductivity (4-probe DC) and Seebeck coefficient were carried out in the oxygen partial pressure range 10^{-15}-10^5 Pa at 700-950^{0}C. The difference between total conductivity values, calculated from impedance spectra and measured by the 4-probe DC technique, was within the limits of experimental uncertainty (1-3%); this suggests that, in the high-temperature range studied in the present work, the grain-boundary resistivity is negligible, in agreement with impedance spectra analysis. Mössbauer spectra were collected in transmission mode using a conventional constant-acceleration spectrometer and a 25 mCi ^{57}Co source in a Rh matrix. The spectra were fitted to Lorentzian lines using a non-linear least-squares method. Estimated deviations for the isomer shift relative to metallic Fe (IS), quadrupole splitting (QS) and full width at half maximum (Γ) are less than 0.02 mm/s, and for relative areas (I) lower than 2%. The oxygen ion transference numbers were determined by the modified Faradaic efficiency (FE) method, taking electrode polarization into account. The FE measurements were performed under zero oxygen chemical potential gradient in air at 700-950^{o}C, and also isothermally at 900^{o}C varying the oxygen partial pressure inside the cell (p_1) with constant oxygen pressure at the external electrode (p_2) equal to 21 kPa. Detailed description of the experimental techniques, used in this work, was published elsewhere.[7-9]

3. Results and discussion

XRD analysis of $La_{10}Si_{6-x}Fe_xO_{27-x/2}$ (x = 1–2) ceramics showed formation of single apatite phases. The unit cell parameters (Table 1) increase with increasing x due to a larger size of Fe^{3+} cations with respect to Si^{4+}. The dilatometric curves of $La_{10}Si_{6-x}Fe_xO_{27-x/2}$ at 100-1000^{o}C are linear, confirming the absence of phase transformations. The substitution of silicon with iron leads to a slight increase of the average thermal expansion coefficients (TECs) calculated from dilatometric data, probably a result of electronic transitions or minor oxygen losses on heating. Nonetheless, the TEC values are relatively low, $(8.2\text{-}9.9)\times10^{-6}$ K^{-1} (Table 1), which is advantageous for high-temperature electrochemical applications.

For $La_{10}Si_{6-x}Fe_xO_{27-x/2}$ system, the incorporation of extra oxygen with respect to the stoichiometric amount, 26 atoms per formula unit, is expected at $x < 2$. The oxygen ionic conductivity should increase with decreasing iron

content due to higher concentration of oxygen interstitials.[4,5] Indeed, the total conductivity of the title materials considerably increases when x decreases (Fig.1); the measurements of transference numbers by the FE technique demonstrated prevailing ionic transport (Table 1). Note that the conductivity of $La_{10}Si_5FeO_{26.5}$ is close to that of 8% yttria-stabilized zirconia[10], one of the most widely used solid electrolytes. The activation energy for ionic conduction in $La_{10}Si_{6-x}Fe_xO_{27-x/2}$ ceramics, calculated by the standard Arrhenius equation, increases on iron doping and varies in the range 81-107 kJ/mol (Table 1).

The Mössbauer spectrum of $La_{10}Si_4Fe_2O_{26}$ consists of two symmetric peaks and thus was fitted by one quadrupole doublet, with IS value characteristic of Fe^{3+} tetrahedrally coordinated by O^{2-} (Table 2). On the contrary, the doublet peaks of $La_{10}Si_{6-x}Fe_xO_{27-x/2}$ (x = 1 and 1.5) are asymmetric. After checking that other effects could not explain this asymmetry[7], a second quadrupole doublet was considered in the analysis of these spectra. While the estimated IS values of the first doublet are close to those of $La_{10}Si_4Fe_2O_{26}$, the second doublet can be attributed to penta-coordinated trivalent iron cations.[9] This suggests that extra oxygen is incorporated in the nearest neighborhood of Fe^{3+}, in agreement with predictions of energy-preferential interstitial positions evaluated by atomistic modeling.[11] The concentration of penta-coordinated Fe^{3+} is quite close to the content of hyperstoichiometric oxygen, increasing when x decreases (Table 2). Mössbauer spectra of the title materials further showed that no tetravalent iron is formed, in contrast to the $La_{9.83}Si_{4.5}Al_{1.5-y}Fe_yO_{26+\delta}$ series[7] where iron doping results in Fe^{4+} formation compensated by extra oxygen intercalation.

The oxygen ion transference numbers (t_o) of $La_{10}Si_{6-x}Fe_xO_{27-x/2}$ with x = 1.0-1.5, determined by the FE technique under oxidizing conditions, are higher than 0.99; Table 1 lists selected examples at 800^0C in air. For $La_{10}Si_4Fe_2O_{26}$, the electronic contribution to the total conductivity is up to 3%. Although electronic transport might be expected to increase when the concentration of variable-valence iron cations increases, the partial electronic conductivity (σ_e) exhibits an opposite trend and correlates with the content of extra oxygen (Table 1). Such a behavior can be explained assuming that the bonding of hyperstoichiometric oxygen in the apatite lattice is weaker than that of anions forming regular $(Si,Fe)O_4$ tetrahedra. In this situation, heating may lead to minor oxygen losses compensated by the generation of n-type electronic charge carriers. In the case of oxygen-stoichiometric $La_{10}Si_4Fe_2O_{26}$, electronic conduction is expected to occur via migration of holes formed due to charge disproportionation of Fe^{3+}; although the concentrations of holes and electrons should be similar, the p-type carriers

typically possess a significantly higher mobility.[12] Decreasing x in $La_{10}Si_{6-x}Fe_xO_{27-x/2}$ apatites should hence increase the role of n-type electronic conduction.

This hypothesis is supported by data on ion transference numbers as a function of the oxygen pressure (Fig.2). For $La_{10}Si_4Fe_2O_{26}$, the t_o values increase when $p(O_2)$ decreases, unambiguously indicating that the electronic conduction under oxidizing conditions is predominantly p-type. These variations can be described by the analytical solution[7] of Wagner equation for ion transference numbers, averaged under an oxygen partial pressure gradient from p_1 to p_2:

$$\overline{t_O}(p_2,p_1) = -m \cdot \ln \frac{k_1 \cdot p_2^{-1/m} + 1}{k_1 \cdot p_1^{-1/m} + 1} \cdot \left(\ln \frac{p_2}{p_1} \right)^{-1} \qquad (1)$$

where the ionic conductivity (σ_o) is essentially $p(O_2)$-independent, the p-type electronic conductivity (σ_p) is predominant with respect to n-type and follows a standard power dependence $\sigma_p = \sigma_{p0} \times p(O_2)^{1/m}$ with m>0, and $k_1=\sigma_o/\sigma_{p0}$. The fitting results are shown in Fig. 2 by solid lines. Both $La_{10}Si_4Fe_2O_{26}$ and $La_{10}Si_{4.5}Fe_{1.5}O_{26.25}$ exhibit positive m values; for the latter composition, however, 1/m is close to 0, thus indicating that the concentrations of n- and p-type charge carriers are comparable.

The $p(O_2)$ dependencies of total conductivity and Seebeck coefficient (α) confirm that, under oxidizing conditions, $La_{10}Si_{6-x}Fe_xO_{27-x/2}$ are solid electrolytes (Fig. 3). At $p(O_2) > 10^{-8}$ Pa, the conductivity remains essentially independent of the oxygen pressure. The Seebeck coefficient in oxidizing atmospheres is positive; the slope of α *vs. ln p(O₂)* is close to (–R/4F), the theoretical value for a pure solid electrolyte. Under reducing conditions, however, the conductivity of $La_{10}Si_5FeO_{26.5}$ starts to decrease, while the thermopower variations suggest that the ionic transport is still dominant. Such a tendency is due to decreasing oxygen ionic charge carrier concentration. The conductivity of $La_{10}Si_4Fe_2O_{26}$ slightly increases on reduction, whereas the Seebeck coefficient shows a behavior indicative of increasing n-type electronic transport.[12] Most likely, the latter trend masks a drop of ionic conduction, expected when the oxygen content is lower than stoichiometric.[4,5] If compared to the $La_{9.67}Si_5AlO_{26}$ apatite where no variable-valence cations are incorporated into the lattice, the stability of all Fe-substituted phases in reducing environments is rather poor.

In summary, $La_{10}Si_{6-x}Fe_xO_{27-x/2}$ (x = 1.0-1.5) ceramics possess ionic conductivity comparable to that of yttria-stabilized zirconia, moderate thermal expansion, and electron transference numbers lower than 0.01 under oxidizing conditions. Taking into account that the component costs of the Fe-substituted silicates are relatively low, these

phases deserve further attention for practical applications. Main approaches to improve their performance may include a slight increase of the oxygen hyperstoichiometry to achieve optimum interstitial concentration and minor doping by higher-valence cations in order to suppress oxygen content variations at low $p(O_2)$.

Acknowledgements

This work was supported by the FCT, Portugal (POCTI program and Projects SFRH/BD/6595/2001 and SFRH/BPD/9312/2002) and the NATO Science for Peace program (project 978002). Helpful discussions and experimental contributions, made by M. Patrakeev, E. Tsipis, A. Yaremchenko and N. Vyshatko, are gratefully acknowledged.

References

1. Steele, B. C. H., Material science and engineering: the enabling technology for the commercialization of fuel cell systems. *J. Mater. Sci*., 2001, **36**, 1053-1068.
2. Nakayama, S., Kageyama, T., Aono, H. and Sadaoka, Y., Ionic conductivity of lanthanoid silicates, $Ln_{10}(SiO_4)_6O_3$ (Ln = La, Nd, Sm, Gd, Dy, Y, Ho, Er and Yb). *J. Mater. Chem*., 1995, **5**, 1801-1805.
3. Nakayama, S. and Sakamoto, M., Electrical properties of new type high oxide ionic conductor $RE_{10}Si_6O_{27}$ (RE = La, Pr, Nd, Sm, Gd, Dy). *J. Eur. Ceram. Soc.*, 1998, **18**, 1413-1418.
4. Tao, S. and Irvine, J. T. S., Preparation and characterization of apatite-type lanthanum silicates by a sol-gel process. *Mat. Res. Bull.*, 2001, **36**, 1245-1258.
5. Sansom, J. E. H., Richings, D. and Slater, P. R., A powder neutron diffraction study of the oxide-ion-conducting apatite-type phases, $La_{9.33}Si_6O_{26}$ and $La_8Sr_2Si_6O_{26}$. *Solid State Ionics*, 2001, **139**, 205-210.
6. McFarlane, J., Barth, S., Swaffer, M., Sansom, J. E. H. and Slater, P. R., Synthesis and conductivities of the apatite-type systems, $La_{9.33+x}Si_{6-y}M_yO_{26+z}$ (M = Co, Fe, Mn) and $La_8Mn_2Si_6O_{26}$. *Ionics*, 2002, **8**, 149-154.
7. Shaula, A. L., Kharton, V. V., Waerenborgh, J. C., Rojas, D. P., Tsipis, E. V., Vyshatko, N. P., Patrakeev, M. V. and Marques, F. M. B., Transport properties and Mössbauer spectra of Fe-substituted $La_{10-x}(Si,Al)_6O_{26}$ apatites. *Mater. Res. Bull.*, 2004, **39**, 763-773.
8. Patrakeev, M. V., Mitberg, E. B., Lakhtin, A. A., Leonidov, I. A., Kozhevnikov, V. L., Kharton, V. V., Avdeev, M. and Marques, F. M. B., Oxygen nonstoichiometry, conductivity and Seebeck coefficient of $La_{0.3}Sr_{0.7}Fe_{1-x}Ga_xO_{2.65+\delta}$ perovskites. *J. Solid State Chem*., 2002, **167**, 203-213.
9. Waerenborgh, J. C., Figueiredo, F. M., Frade, J. R., Colomer, M. T. and Jurado, J. R., Fe^{4+} content and ordering of anion vacancies in partially reduced $AFe_xTi_{1-x}O_{3-y}$ (A = Ca, Sr; $x \leq 0.6$) perovskites. An Fe-57 Mössbauer spectroscopy study. *J. Phys.-Cond. Matter*, 2001, **13**, 8171-8187.
10. Mori, M., Abe, T., Itoh, H., Yamomoto, O., Takeda, Y. and Kawahara, T., Cubic-stabilized zirconia and alumina composites as electrolytes in planar type solid oxide fuel cells. *Solid State Ionics*, 1994, **74**, 157-164.
11. Tolchard, J. R., Islam, M. S. and Slater, P. R., Defect chemistry and oxygen ion migration in the apatite-type materials $La_{9.33}Si_6O_{26}$ and $La_8Sr_2Si_6O_{26}$. *J. Mater. Chem*., 2003, **13**, 1956-1961.
12. Mizusaki, J., Sasamoto, T., Cannon, W. R. and Bowen, H. K., Electronic conductivity, Seebeck coefficient, and defect structure of $LaFeO_3$. *J. Am. Ceram. Soc.*, 1982, **65**, 363-368.

Table 1.

Properties of Fe-containing apatite ceramics

Composition	Sintering temperature, °C	Space group	Unit cell parameters		ρ_{exp}, g/cm^3	Relative density, %
			a, nm	c, nm		
$La_{10}Si_5FeO_{26.5\pm\delta}$	1500	$P6_3/m$	0.9757(3)	0.7255(1)	5.51	98.8
$La_{10}Si_{4.5}Fe_{1.5}O_{26.25\pm\delta}$	1550	$P6_3/m$	0.9765(8)	0.7255(7)	5.50	98.3
$La_{10}Si_4Fe_2O_{26\pm\delta}$	1600	$P6_3$	0.9788(7)	0.7268(7)	5.53	99.0

Composition	Average thermal expansion coefficient $\bar{\alpha} \times 10^6$, K^{-1}	Transport properties at 800°C in air			Activation energies for ionic transport at 600-1000°C, kJ/mol
		σ_o, S/cm	σ_e, S/cm	t_o	
$La_{10}Si_5FeO_{26.5\pm\delta}$	8.22 ± 0.03	2.3×10^{-2}	9.7×10^{-5}	0.996	81 ± 1
$La_{10}Si_{4.5}Fe_{1.5}O_{26.25\pm\delta}$	8.61 ± 0.03	7.6×10^{-3}	6.0×10^{-5}	0.992	95 ± 2
$La_{10}Si_4Fe_2O_{26}$	9.90 ± 0.01	4.8×10^{-4}	1.4×10^{-5}	0.971	107 ± 4

Table 2.

Parameters estimated from the Mössbauer spectra of the apatite samples at room temperature

Composition	Iron state	IS, mm/s	QS, mm/s	Γ, mm/s	I, %
$La_{10}Si_4Fe_2O_{26}$	Fe^{3+} (CN=4)	0.12	0.69	0.34	~100
$La_{10}Si_{4.5}Fe_{1.5}O_{26.25}$	Fe^{3+} (CN=4)	0.11	0.73	0.39	81
	Fe^{3+} (CN=5)	0.29	0.87	0.31	19
$La_{10}Si_5FeO_{26.5}$	Fe^{3+} (CN=4)	0.11	0.76	0.46	63
	Fe^{3+} (CN=5)	0.29	0.89	0.29	37

Figure captions

Fig.1. Temperature dependence of the total conductivity in air. Data on 8% Y_2O_3 stabilized ZrO_2[10] are shown for comparison.

Fig.2. Dependence of the average ion transference numbers of $La_{10}Si_{4.5}Fe_{1.5}O_{26.25}$ and $La_{10}Si_4Fe_2O_{26}$ on the oxygen partial pressure inside the measuring cells. Solid lines correspond to best fit to Eq. (1).

Fig.3. Oxygen partial pressure dependencies of the total conductivity (A) and Seebeck coefficient (B) of apatite ceramics.

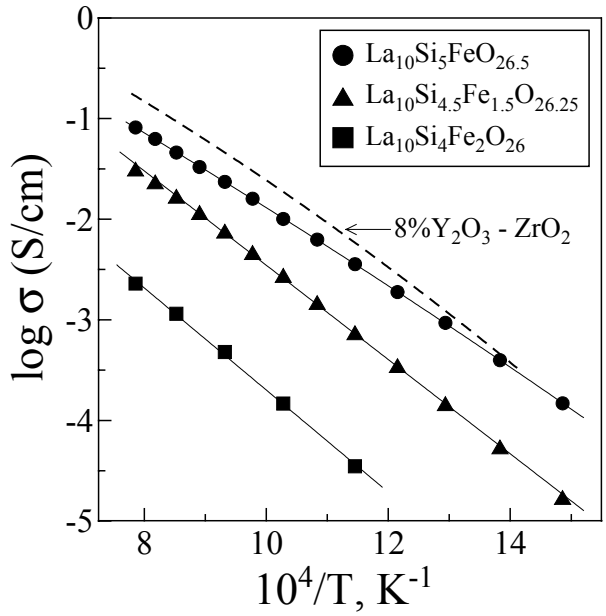
0
-1
-2
-3
-4
-5
8
10
12
14
log σ (S/cm)
10^4/T, K^-1
La10Si5FeO26.5
La10Si4.5Fe1.5O26.25
La10Si4Fe2O26
8%Y2O3 - ZrO2

Fig.1.

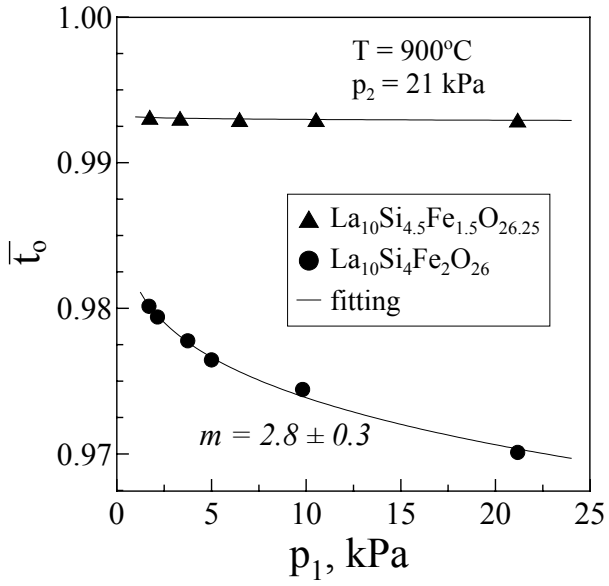
1.00
0.99
0.98
0.97
t_o
T = 900°C
p_2 = 21 kPa
$La_{10}Si_{4.5}Fe_{1.5}O_{26.25}$
$La_{10}Si_4Fe_2O_{26}$
fitting
m = 2.8 ± 0.3
0
5
10
15
20
25
p_1, kPa

Fig.2.

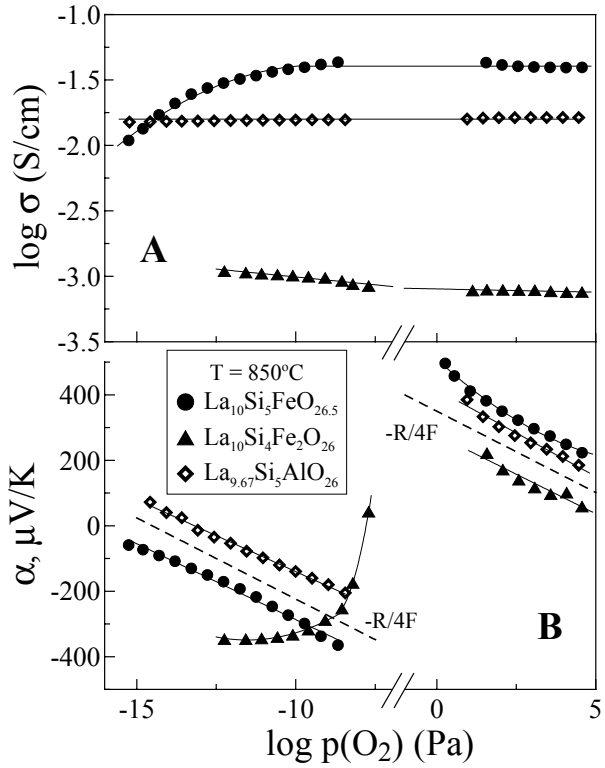
log σ (S/cm)
A
B
T = 850ºC
La10Si5FeO26.5
La10Si4Fe2O26
La9.67Si5AlO26
-R/4F
-R/4F
α, μV/K
log p(O2) (Pa)

Fig.3.